Hindawi
Journal of Spectroscopy
Volume 2023, Article ID 8631288, 16 pages
https://doi.org/10.1155/2023/8631288

Research Article

Considerations in Raman Spectroscopy for Real-Time API Concentration Measurement at Tablet Press Feed Frame

Sumit Kumar,[1] **Zoltan Nagy**,[1] **Gintaras V. Reklaitis**,[1] **and Marcial Gonzalez**[2]

[1]*Davidson School of Chemical Engineering, Purdue University, West Lafayette, Indiana 47907, USA*
[2]*School of Mechanical Engineering, Purdue University, West Lafayette, Indiana 47907, USA*

Correspondence should be addressed to Sumit Kumar; kumar344@purdue.edu

Received 9 September 2022; Revised 9 November 2022; Accepted 11 January 2023; Published 16 February 2023

Academic Editor: Mohd Sajid Ali

Raman spectroscopy is one of the important process analytical technology tools available for implementation in the continuous manufacturing of oral solid dosages. The aim of this study was to investigate several practical considerations in generating real-time measurements using Raman spectrometer at a tablet press feed frame, including the effects of fluorescence interference, photobleaching, feed-frame rpm, and material particle size. Fluorescence, in particular, is a significant drawback of Raman spectroscopy, compared to the use of near-infrared spectroscopy. Potential material sparing strategies were also investigated, including using stationary powders for calibration and isolation of feed-frame materials. Acetaminophen was used as the main active pharmaceutical ingredient (API), and microcrystalline cellulose (MCC) and lactose were used as excipients. The fluorescent behavior of MCC at 785 nm laser wavelength was reported and discussed. Raman spectra of a blend of MCC and acetaminophen and lactose and acetaminophen were collected at the feed frame of the tablet press. A series of preprocessing steps applied to remove the fluorescence interference was found to be effective, including the use of standard normal variate, subtraction of spectra of fluorescent material, baseline correction, and smoothing. Three different PLS models were prepared for different scenarios and their performances were compared. The models were able to predict the concentration of acetaminophen with root mean squared error prediction (RMSEP) of 0.29% w/w when there was no fluorescence interference and 0.57% w/w when there was fluorescence interference in background spectra. The study demonstrated the feasibility of using Raman spectroscopy for API concentration prediction even in the case of fluorescent interference and showed that Raman measurements were robust; that is, they were not much affected by feed-frame rpm and excipient particle size.

1. Introduction

The pharmaceutical industry is dominated by batch manufacturing. However, the limitations of batch manufacturing [1] and the advances in technology have led to an accelerating shift from batch manufacturing to continuous manufacturing (CM) in the industry. These technological advances include advancements in computing and information technology, manufacturing technology, and process analytical technology (PAT). Batch manufacturing processes often come with issues such as longer batch times, higher manual intervention, and scale up related challenges [2]. CM provides a more promising approach to effectively utilize assets and materials by exploiting advanced process design, monitoring, and control [3]. The Food and Drug Administration (FDA) has recognized the benefits of CM in the manufacturing of oral solid dosages (OSDs) and has been encouraging the industry towards this mode of manufacturing across product firms [1].

Important components in implementing the CM strategy in the manufacturing of OSDs are as follows: 1. Real-time measurement and monitoring, 2. process control, 3. fault detection, 4. diagnosis of exceptional events, and 5. tracking and isolation of noncompliant products [4]. PAT implementation is essential for all the abovementioned components [5, 6]. The concentration of active pharmaceutical ingredients (API) is one of the most important CQA in the manufacturing of OSD as it determines the amount of drug

substance present in the tablet [7]. The issue of overdosing and underdosing can be mitigated by correctly quantifying the API concentrations using appropriate PAT. The PAT tools also allow real-time monitoring of a continuous flow of material without the need for the physical sampling of powders as measurement can be done using a contactless probe.

Reflectance spectroscopy is one of the most widely used PAT in the industry with near infrared (NIR) and Raman, the two most important spectroscopy tools [8–11]. Of the two, the implementation of NIR in product research and manufacturing of OSD is far more prevalent than the implementation of Raman spectroscopy [12, 13]. The main reasons behind this are that the laser source in Raman requires additional safety considerations while handling at the manufacturing floor and the probe may require the elimination of ambient light. In addition, the high energy of the Raman lasers can degrade the samples being measured. Also, some materials can exhibit fluorescence and photobleaching phenomena and that can obscure the Raman spectra. Moreover, Raman typically requires longer exposure and sampling times compared to NIR [14]. However, there are many important advantages of Raman spectroscopy [15]: it provides excellent molecular specificity [16], it has better sensitivity [17] and thus can be used for identification and quantification at low concentrations [18, 19], and it is not affected by the presence of aqueous components such as water molecules [20].

In continuous OSD manufacturing, API concentration measurements are most useful in two process locations: after the main blending step and at the tablet press. In the former case, the measurement can be used in the control of the ratio of the flows from the API and excipient loss-in-weight feeders, thus allowing compensation for any drift or deviations in the flows provided by the individual feeders. API measurement at the tablet press provides information that is representative of the API concentration of the final tablets and can inform the decision to reject out of specification tablets. In principle, this measurement can also be a fed-back upstream for ratio control; however, the control response will be delayed by the residence time of the intervening unit operations. The API composition measurement at the tablet press can be taken either in the tablet press hopper or in the feed frame. Real-time composition measurement of tablets issuing from the press is not feasible, given the high tablet production rates. Measurement of the API concentration at the feed frame location has the advantage that, short of measurements in the die, this is the final mixing stage before tablet production and thus is often recommended [21, 22]. In this study, we investigate the use of Raman reflectance spectroscopy as a PAT for API concentration monitoring with the sampling location at the feed frame of a continuous tableting line.

Raman spectroscopy is based on the scattering phenomenon that occurs due to collisions between photons and molecules. Raman spectroscopy provides vibrational information about the chemical constituents of the sample and imposes a change in the polarizability of a vibrational group within a molecule. Most photons colliding with molecules do not change their energy and give rise to Rayleigh scattering. However, a few photons exchange energy with the molecules during the collision and give rise to Raman scattering. The scattered light with energy less than the incident light is called "Stokes Raman scattering" and with energy higher than the incident light is called "anti-Stokes Raman scattering" [23, 24]. The probability of occurrence of Stokes scattering is higher than that of anti-Stokes scattering. The transition from one molecular energy level to another can occur between different electronic, vibrational, or rotational energy levels, but the vibrational energy level changes are the most likely changes that occur in Raman scattering. The spectra contain fundamental signatures of various chemical bonds within the molecule and make the identification of a chemical entity easier. Raman has higher chemical selectivity and gives sharp peaks.

The Raman signals are weak signals—stokes and anti-stokes—and many times strong fluorescence broadband appears in the same region that affects the background and obscures the Raman spectra. Fluorescence masks the Raman spectra and is one of the biggest drawbacks of Raman spectroscopy. It occurs when the molecule excites to an energy state higher than the electronic excited state and decays to the lowest vibrational level of that electronic state via radiation-less transitions and then emits radiations [25]. Photobleaching is another phenomenon where the fluorophore starts losing its fluorescence, and the intensity of fluorescence broadband reduces over time. This results in the reduction in peak intensity of the overall Raman signals and affects the quantitative calibration model performance. Many pharmaceutical excipients have cellulose products that may contain fluorophores such as lignin [14, 26]. Acquisition of good quality spectra is important for the identification and quantification of material of interest in a mixture of powders.

Fluorescence interferences can be reduced by choosing a laser of appropriate wavelength so that the Raman signal is located in the ultraviolet (UV) or NIR ranges, as the Raman signal will be in an energy level lower than that of emitted fluorescence [27]. The laser photon in this range does not have enough energy to excite the fluorophore. Raman scattering depends on the excitation wavelength to the fourth power whereas the intensity linearly affects the Raman signal [28]. However, in a mixture of different materials, it is difficult to find an optimum laser wavelength where no fluorescence is observed as different materials fluoresce at different ranges of wavelengths. Excitation at 785 nm (red spectral region) has been selected as an optimal wavelength in many modern Raman spectrometers considering both the fluorescence at higher wavelengths and loss of signals at lower wavelengths [29].

One way of reducing the fluorescent background is by using shifted-excitation Raman difference spectroscopy (SERDS), where the Raman signal is collected at two near neighbour wavelengths and then subtracted to have the improved Raman spectra [29]. However, this requires spectrometer setup to be capable of having the laser adjusted to different wavelengths, which is difficult to implement in real-time process monitoring scenarios. In this study, we

investigate the use of Raman spectroscopy to measure API concentration in a moving powder blend consisting of acetaminophen and several excipients. The first objective is development of a novel way of removing the fluorescent background interference, one of the major drawbacks in the implementation of Raman spectroscopy. The focus of the current study is to eliminate the undesired fluorescent background from the Raman spectra of the blend of powders and explain the mathematical preprocessing strategy used. The second objective is to develop new ways of building calibration models using reduced amounts of materials. Our study includes alternative strategies for collecting data for building calibration models. The study then compares the model performance using these novel methods. The third objective is to assess the impact of sampling on photobleaching. The work also provides a unique approach to reduce the impact of photobleaching.

The present study evaluates other considerations in the implementation of Raman spectroscopy as well. First, the PLS model [30] is prepared in two scenarios: when there is minimal fluorescence and when there is high fluorescence, and the model performance in both cases is compared. Second, the Raman spectra for stationary and flowing powders, having different API concentrations, inside the feed frame of the tablet press are studied. Models prepared using stationary and flowing powder inside the feed frame are compared. Lastly, the effect of change in feeder RPM on the model predictions is studied. The authors understand that this is the first work that provides these novel ways of correcting photobleaching and fluorescence effects in the pharmaceutical excipient and evaluates different considerations in implementing Raman spectroscopy. The work will help in the broader implementation of Raman spectroscopy in real-time monitoring of API concentration, even in situations where there is a fluorescence background. Model building with lesser material can be important in industrial situations where only a limited amount of API is available or where the API cost is high. The approaches studied here could also reduce the need for multiple laser sources with different wavelengths to reduce the impact of fluorescence.

2. Material and Methods

2.1. Materials. The materials used in the study are acetaminophen (APAP), lactose, microcrystalline cellulose (MCC), magnesium stearate, and silica. Powdered blends of API, i.e., APAP and excipients are prepared for analysis by Raman spectroscopy at the feed frame location of the tablet press. Acetaminophen Grade 0048, purchased from Mallinckrodt (Raleigh, NC), is used as API. Avicel microcrystalline cellulose Grade PH-102 (MCC-102) and Grade PH-200 (MCC-200), purchased from FMC BioPolymer (Philadelphia, PA), are used as filler excipients. Lactose monohydrate Grade 310, purchased from Kerry Inc. (Jackson, WI), is used as a filler excipient. Magnesium Stearate (MgSt) is used as a lubricant to prevent adhesion during tableting in a rotary tablet press. Silica is the flowing agent used to improve the powder flow in the direct compaction line.

2.2. Preparation of Blends. Raman spectra of pure materials and of blends of API and excipients are recorded for this study. The blends are prepared by charging the known quantities of APAP, lactose or MCC, silica, and MgSt in the bin blender from Tote systems. A total of 1 kg of raw materials (RM) is charged into the batch blender and rotated at the RPM of 15 for 20 minutes for uniform mixing. The material is then unloaded and charged to the hopper of the tablet press. For one set of studies, the APAP concentration is varied from 8% weight by weight (w/w) to 15% w/w and lactose is varied from 91.3% w/w to 84.3% w/w as shown in Table 1.

For the next set, MCC is used as the main filler excipient. The remaining materials are APAP, MgSt, and silica (Table 2). The APAP concentration is varied from 8% w/w to 15% w/w. The blending process is the same as explained above.

2.3. Experimental Procedure. One kilogram of each nominal blend of different drug compositions (8 to 15% w/w) of APAP in the excipients is prepared and blended as described above. The blended material is charged to the hopper of the tablet press. The tablet press is the unit operation widely used to compress powder blends into tablets. It consists of a hopper, a feed frame, and multiple dies, all operating in an integrated fashion at high speeds to produce over a million tablets per hour in commercial-scale tablet presses. The hopper of the tablet press discharges the homogeneous blend into the feed frame. The feed frame consists of a dual paddle force feeder which mixes and distributes the powder and ensures that the dies are filled uniformly. A tablet is formed by the combined action of upper and lower pistons, called punches, on the powder in the die. The experimental work reported here uses a Natoli—NP 400—tablet press with 22 stations. The material flows from the custom-made vertical hopper and the feed frame before being compacted (Figures 1(a) and 1(b)). Pure components materials and different blends are charged to the feed frame of the tablet press. Spectroscopic measurements are made on both stationary and moving powder at feed frame locations (Figure 1(c)). The paddle speed is varied from low to high to generate the data needed to understand the impact of blend flow rate on spectral data collected. The required spectral data from different experiments are collected over multiple days. A special strategy was used to minimize the material required to take the Raman spectra of materials in feed frame for longer times. The paddles of the feed frame were rotated at 40 RPM to collect the spectra of flowing powder inside the feed frame but the turret was not rotated. Hence, we were able to collect the spectra for any required duration with a limited quantity of powder inside the feed frame. Once the spectra collection is completed, the material is unloaded from the bottom of the feed frame and almost 90% of the material charged can be recovered for any future reuse. If the turret was also rotated with the feeder (as in a normal tablet compression process using tablet press), then approximately 1 kg of material would have been consumed in every 10-minute run for each blend prepared. This strategy helped in measuring the spectra of flowing powder without sacrificing

Table 1: Blend composition for APAP in lactose.

Material	Blend percent (w/w)							
APAP	8	9	10	11	12	13	14	15
Lactose	91.3	90.3	89.3	88.3	87.3	86.3	85.3	84.3
MCC	0	0	0	0	0	0	0	0
MgSt	0.5	0.5	0.5	0.5	0.5	0.5	0.5	0.5
Silica	0.2	0.2	0.2	0.2	0.2	0.2	0.2	0.2

Table 2: Blend composition for APAP in MCC.

Material	Blend percent (w/w)							
APAP	8	9	10	11	12	13	14	15
Lactose	0	0	0	0	0	0	0	0
MCC	91.3	90.3	89.3	88.3	87.3	86.3	85.3	84.3
MgSt	0.5	0.5	0.5	0.5	0.5	0.5	0.5	0.5
Silica	0.2	0.2	0.2	0.2	0.2	0.2	0.2	0.2

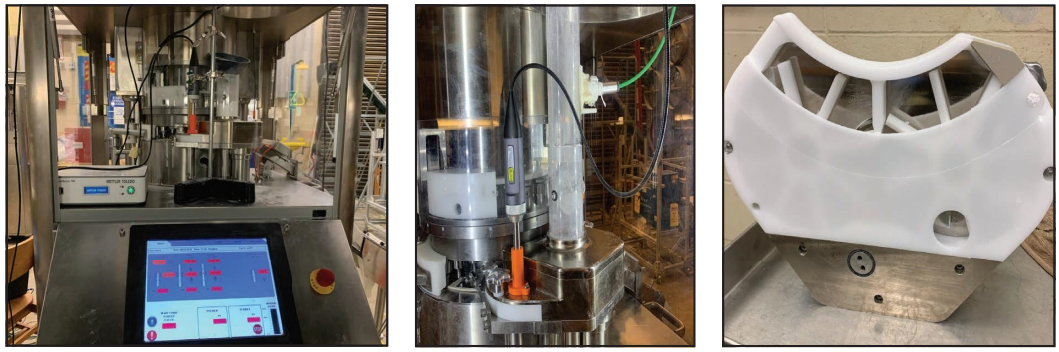

(a) (b) (c)

Figure 1: (a) Tablet press and Raman spectrometer, (b) 3D printed sensor holder, and (c) feed-frame of Natoli NP 400 tablet press.

much of the materials and can be used in scenarios where limited quantities of raw material, especially APIs, are available such as during the early stages of development. The same strategy was used to minimize the powder usage for calibration studies. This is a new innovative method of performing model calibration at the feed frame of tablet press with limited material. The Raman spectra of stationary powder at the feed frame are also collected for comparison study by stopping the feeder paddles. The steps are repeated for the remaining APAP concentrations as well.

The Raman spectrometer is a ReactRaman 785 system (Figure 1(a)) with 100—3200 cm^{-1} optical range (1 cm^{-1} spacing) and 785 nm excitation wavelength. It was operated at 400 mW at source. The spectrometer is provided by Mettler Toledo. It uses a class 3B laser source, and beam diameter of the noncontact probe is 90 μm. The exposure time is varied to set the signal saturation at 50–75%. Raman sensor is located at the feed frame of the tablet press (Figure 1(a)). The sensor holder was custom-fabricated for this project using the 3D printing facilities at Purdue to appropriately present the Raman probe to the powders inside the feed frame location of the tablet press. The sampling time per spectra collection varies from 0.5 to 3 seconds. The software used for data processing and model building is the iC Raman software provided by Mettler Toledo. A minimum of three spectra are collected, and the integration time is 4 seconds. Hence, for a setting of 1 second per spectra, considering 3 spectra, the time for total spectra collection is 3 seconds and integration time is 4 seconds making the total time for one final spectra recorded as 7 seconds.

2.4. Multivariate Data Analysis. Quantitative data analysis of the Raman spectra is done by measuring the peak areas and using a multivariate data analysis method to translate the spectral data into the concentration of the molecule of interest. Model development is done by performing calibration and validation steps using Raman spectra that are collected at different blend compositions. Spectral data collected at the feed frame is pretreated using the appropriate spectral preprocessing method, the rationale for which is explained in the results section. After preprocessing, partial least square (PLS) [30] models are prepared to predict the API concentration from the spectral data measured, and the best model is selected based on the R^2, root mean squared error calibration (RMSEC), root mean squared error cross-validation (RMSECV, equation (1)), and root mean squared error prediction (RMSEP, equation (2)) values. The

iC Raman 7.0 software package is used to prepare the PLS models.

$$\text{RMSECV} = \sqrt{\frac{\sum \left(\hat{y}_i - y_i\right)^2}{n - N}}, \quad (1)$$

$$\text{RMSEP} = \sqrt{\frac{\sum \left(\hat{y}_i - y_i\right)^2}{n}}. \quad (2)$$

Here, y_i is the measured or known API concentration, $\hat{y}_i$ are the API concentrations predicted by the model, n is the number of samples under consideration, and N is the number of factors used in model [14].

3. Results

After completing the material blending and spectra collection, all the experiments are analyzed, and the results are discussed below.

3.1. Spectra of Individual Materials. The individual materials are all analyzed, and the Raman spectra of the pure components are shown in Figures 2(a)–2(f). Raman spectra of all but one ingredient have sharp peaks as expected. The peak intensities also remain constant with time. But the Raman spectra of MCC behaved differently (Figures 2(c) and 2(f)). The peaks are not sharp, and the overall spectra is obscured. Also, the peak intensity does not remain constant; rather, it reduces with time and then plateaus. Such unusual behavior of MCC spectra is attributed to the fluorescent nature of the MCC at the given 785 nm laser source of the Raman spectrometer. Similar behavior is observed with the MCC blends. Such behavior hampers the correct peak identification and quantification in predicting the API concentration.

This obscure behavior in Raman spectra is observed not only in the MCC spectra but also in the spectra of blends having the MCC at lower concentrations. The behavior of the Raman spectra where the peak intensity is reducing with time can be attributed to the phenomenon of photobleaching in fluorescent material. This fluorescent behavior of MCC is verified by comparing the Raman spectra of two different MCC grades, MCC 200 and MCC 102. These two grades have different particle sizes but exhibit similar fluorescence, as shown in Figure 3. The spectra overlap properly, and the intensity of the peaks reduces with time in both the cases (Figures 3(b) and 3(c)).

Three spectra, all having the same 10% w/w APAP but varying amounts of MCC, are shown in Figure 4(a). The green one has no MCC and only lactose as filler excipient, the blue has 90% w/w MCC, and the yellow has 40% w/w MCC. The effect of contributions from MCC can be easily realized in these spectra where only the green one exhibits clear and sharp APAP peaks even though all three have the same 10% w/w of APAP in the blends.

The fluorescence is a broadband peak. The presence of fluorescent material affects the important individual peak identification for the different ingredients and affects the signal to noise ratio and thus directly affects the quantitative analysis to convert the spectral data into important CQAs such as API concentration measurement using mathematical models. Next, we outline a procedure for deriving maximum information from the obscured Raman spectra and for properly preprocessing the raw spectra to extract the Raman spectra of material of interest from the spectra of a mixture of materials having fluorescence.

3.2. Spectral Correction to Remove the Fluorescence Background. Raw spectra and surface plot of a blend of 10% w/w APAP in MCC (89.3% w/w), magnesium stearate (0.5% w/w), and silica (0.2% w/w) at the feed frame of tablet press are shown in Figures 4(b) and 4(c), respectively. Acetaminophen peaks are sparingly visible and are overshadowed by the fluorescent broadband. The two spectra in Figure 4(b) are of the same material inside the feed frame taken at a gap of 2 minutes. The dip in the intensity in a span of 2 minutes is due to the photobleaching behavior.

First, the SNV correction is applied. It is useful to standardize different spectra if the raw peak intensity is not of much importance. Here, the individual data points are subtracted from the mean and then divided by the standard deviation of the data set. As the intensity of all peaks gets reduced relatively with time in the fluorescent material, such correction helps in making the individual peak heights relatively stable with respect to time. This is the first of the several preprocessing steps carried out. The resultant spectra after correction are shown in Figures 4(d) and 4(e). The SNV correction also corrects for the photobleaching effect (explained in Section 3.3).

Next, solvent subtraction is done to remove the contribution of MCC. Raman spectra of pure MCC is taken at the same location inside the feed frame under the same conditions. The recorded spectra of pure MCC are then subtracted from the spectra of the blends. The resultant spectra are shown in Figure 5(a). This step improves the visibility of the APAP peaks.

Next, the spectra is corrected for baseline. Baseline correction schemes allow for complex baseline components, such as linear, quadratic, or other functions to be eliminated. The baseline corrected spectra are shown in Figure 5(b).

Next, smoothing is applied to remove spectral disturbances in the spectra by preprocessing steps as well as to mitigate the disturbances imparted by the spectrometer itself. This step should be carried out with caution so as to verify that important signals are not lost in the smoothing process. In the current scenario, 21 points smoothing is applied and then the spectra are normalized (Figure 5(c)).

Mathematical preprocessing such as 1^{st} and 2^{nd} derivatives can also be applied to enhance the peaks of interest. Finally, after all the required preprocessing, the Raman spectra of the ingredient of interest, APAP, is extracted and compared to the pure APAP spectra and spectra of 10% w/w APAP in lactose where no fluorescence is observed. The comparison shows that important peaks are preserved and the molecular signature of APAP can be analyzed to identify the important peaks (Figure 5(d)). The same steps are

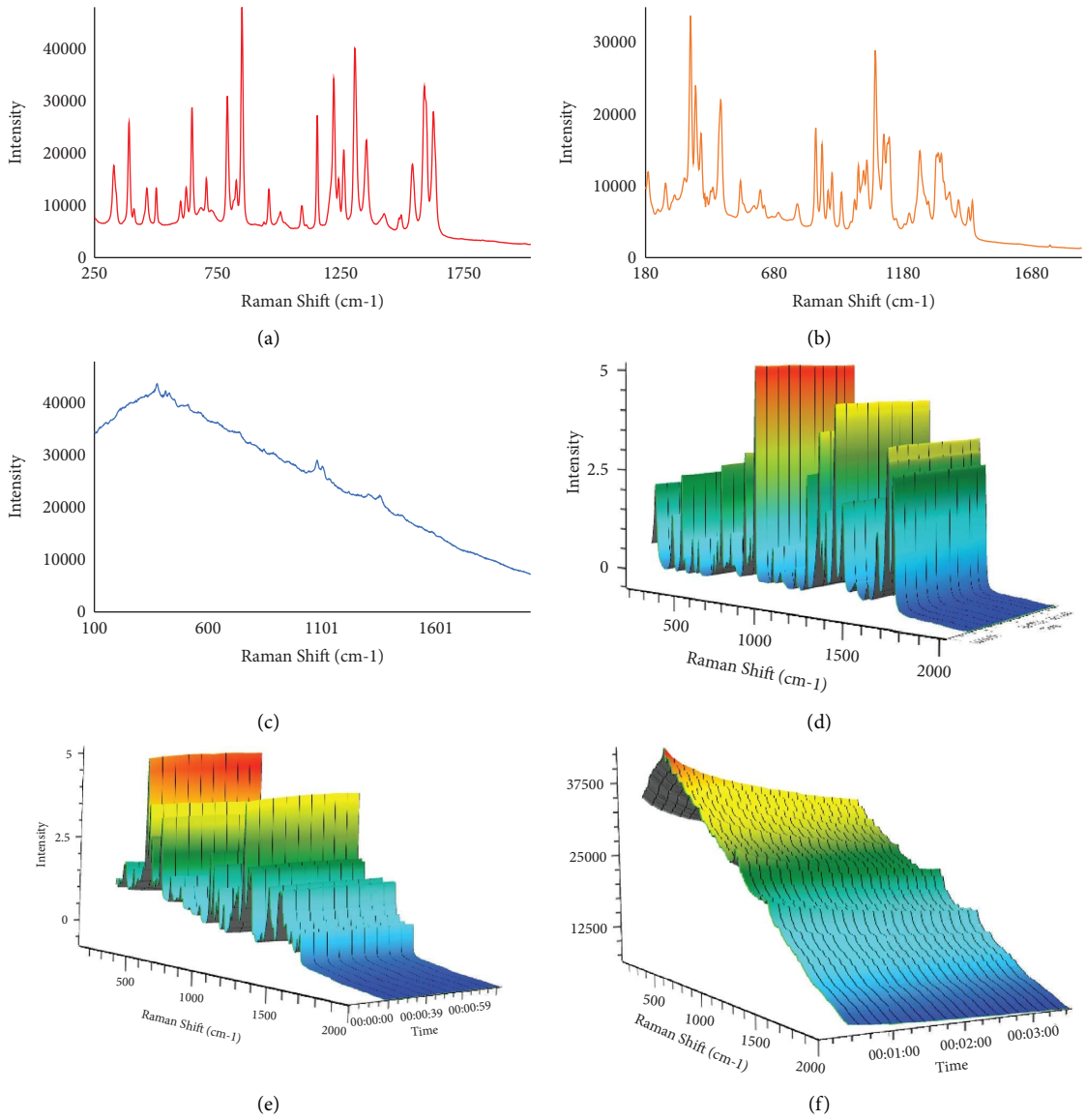

Figure 2: (a) Raman spectra of APAP, (b) Raman spectra of lactose, (c) Raman spectra of MCC, (d) surface plot of Raman spectra of APAP, (e) surface plot of Raman spectra of lactose, and (f) surface plot of Raman spectra of MCC.

followed in the later section while preparing the PLS models to predict the APAP concentration in the blend of different solids in real-time.

All the spectra correction steps can be summarized as follows: (1) raw spectra collection, (2) SNV correction, (3) subtraction of spectra of pure fluorescent material, (4) baseline correction, and (5) smoothing and normalization.

3.3. Correction for Photobleaching. Two strategies are tested to reduce the impact of photobleaching which causes a reduction in the intensity of Raman signals over time. First, mathematical preprocessing using SNV correction is tested. Second, the sampling plan is changed. SNV standardizes different spectra with respect to mean and variations and removes the issue of dropping peak intensities with time (Figure 6(a)). Also, as the issue of photobleaching arises due to the same sample imparting fluorescence being irradiated for a prolonged time, sampling of the flowing powder could mitigate this issue. Raman spectra of the same 10% w/w APAP in MCC for stationary and flowing powders are compared, and as anticipated, the issue of photobleaching is largely reduced with flowing powders (Figure 6(b)).

3.4. Effect of Powder Flow on the Raman Spectra. This comparison is done to understand the difference in the Raman spectra which is collected from stationary powder vs. from flowing powder. This may help in reducing the efforts and materials required for the calibration experiments of the model. Comparison on the static vs. flowing Raman signals for 8% w/w, 10% w/w, and 12% w/w APAP in lactose is shown in Figures 6(c)–6(e), respectively. As can be observed, the spectra are similar and there is no significant difference

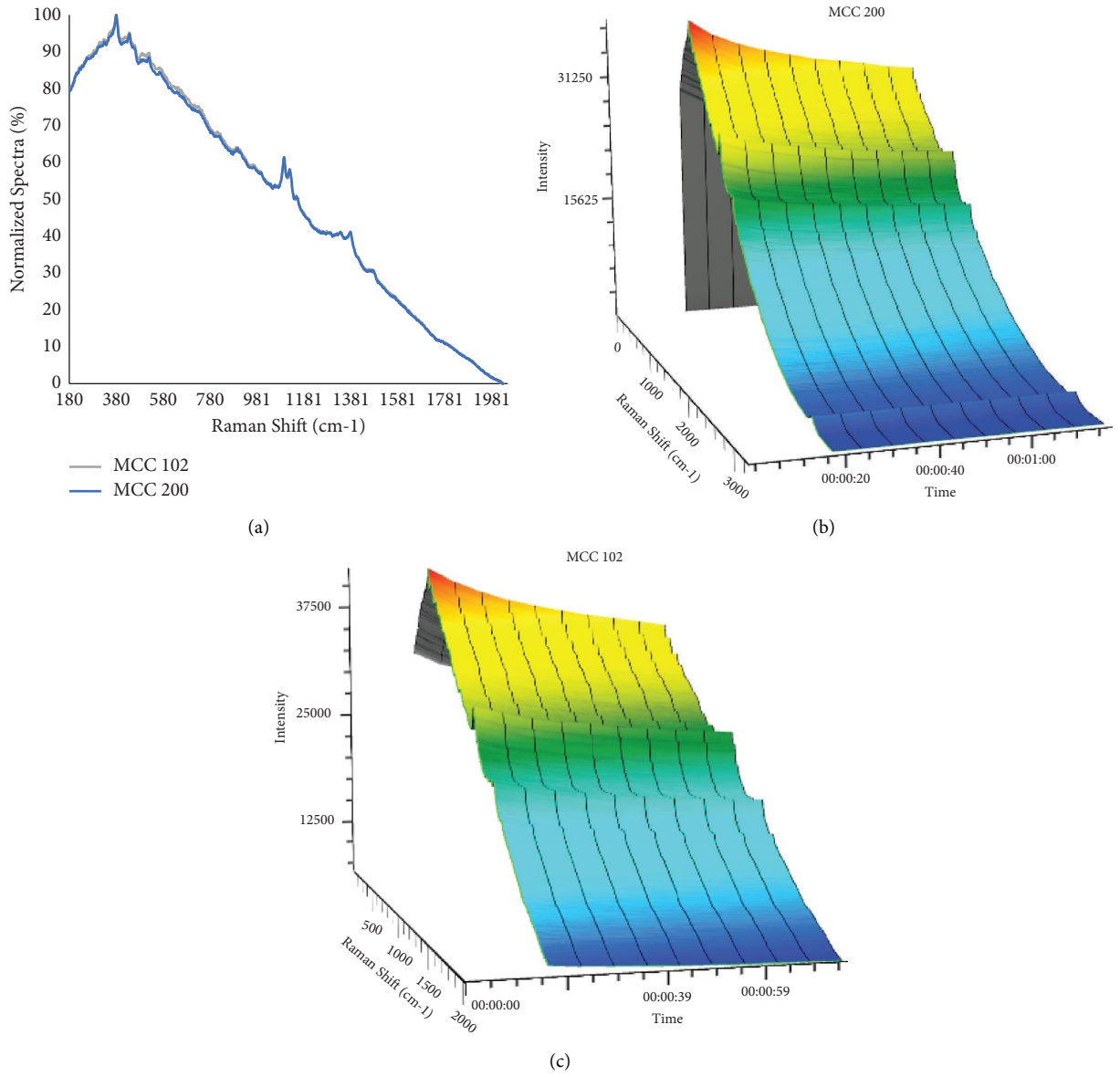

Figure 3: (a) Raman spectra of MCC 200 and MCC 102, (b) surface plot of Raman spectra of MCC 200, and (c) surface plot of Raman spectra of MCC 102.

between them. The correlation coefficient between the spectra is above 0.99. These results suggest that Raman spectra of stationary powders could also be utilized for calibration model preparation. This proposition is tested in the later section.

3.5. PLS Model for Three Different Experiment Data Sets. After gaining the understanding of different aspects of spectra collection at the feed frame of tablet press, the knowledge is applied to build accurate partial least square (PLS) models to predict the API concentration in real-time. The models are prepared by collecting the Raman spectra of the flowing powder and stationary powder inside the feed frame of the tablet press. Each of the models is developed using a total of 120 Raman spectra. Fifteen calibration spectra are collected for each of the blends having the following eight concentrations: 8%, 9%, 10%, 11%, 12%, 13%, 14%, and 15% w/w APAP. The following scenarios are considered:

3.5.1—Blend of APAP and lactose (no fluorescence) with flowing powder inside feed frame

3.5.2—Blend of APAP and lactose (no fluorescence) with stationary powder inside feed frame

3.5.3—Blend of APAP and MCC (fluorescent material) with stationary powder inside feed frame

3.5.1. PLS Model for acetaminophen in lactose Using Flowing Powder. In the first set of experiments, APAP concentration is varied with the main excipient lactose. Following concentrations of APAP in lactose (%w/w) blends are used—8%,

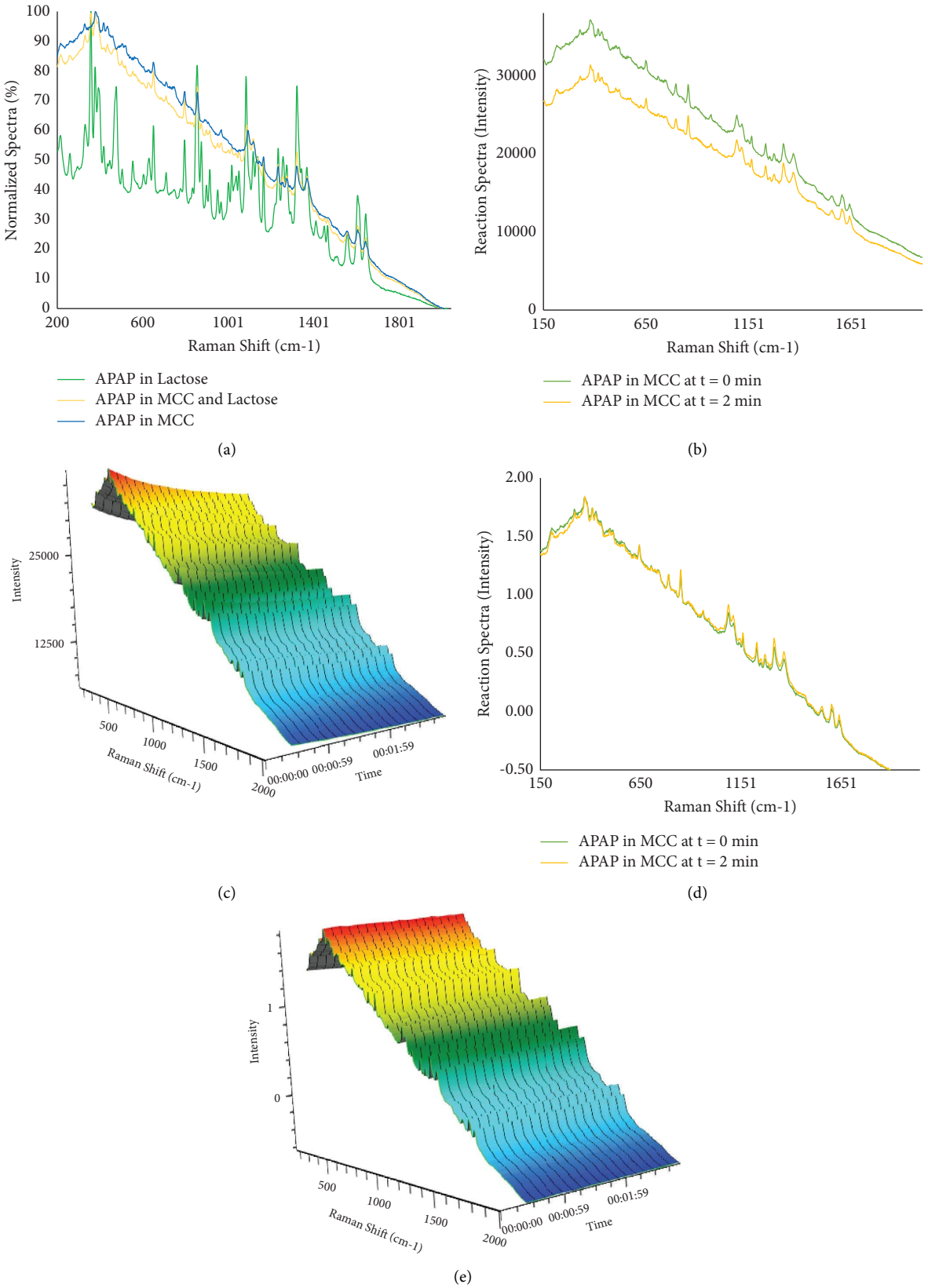

Figure 4: (a) Raman spectra of 10% APAP in only lactose (green), only MCC (blue) and in the mixture of MCC and lactose (yellow), (b) Raman spectra of 10% APAP in MCC at $t = 0$ minutes and $t = 2$ minutes, (c) surface plot of Raman spectra of 10% APAP in MCC showing bleaching over time, (d) Raman spectra of 10% APAP in MCC at $t = 0$ minutes and $t = 2$ minutes after SNV correction, and (e) surface plot of Raman spectra of 10% APAP in MCC after SNV correction.

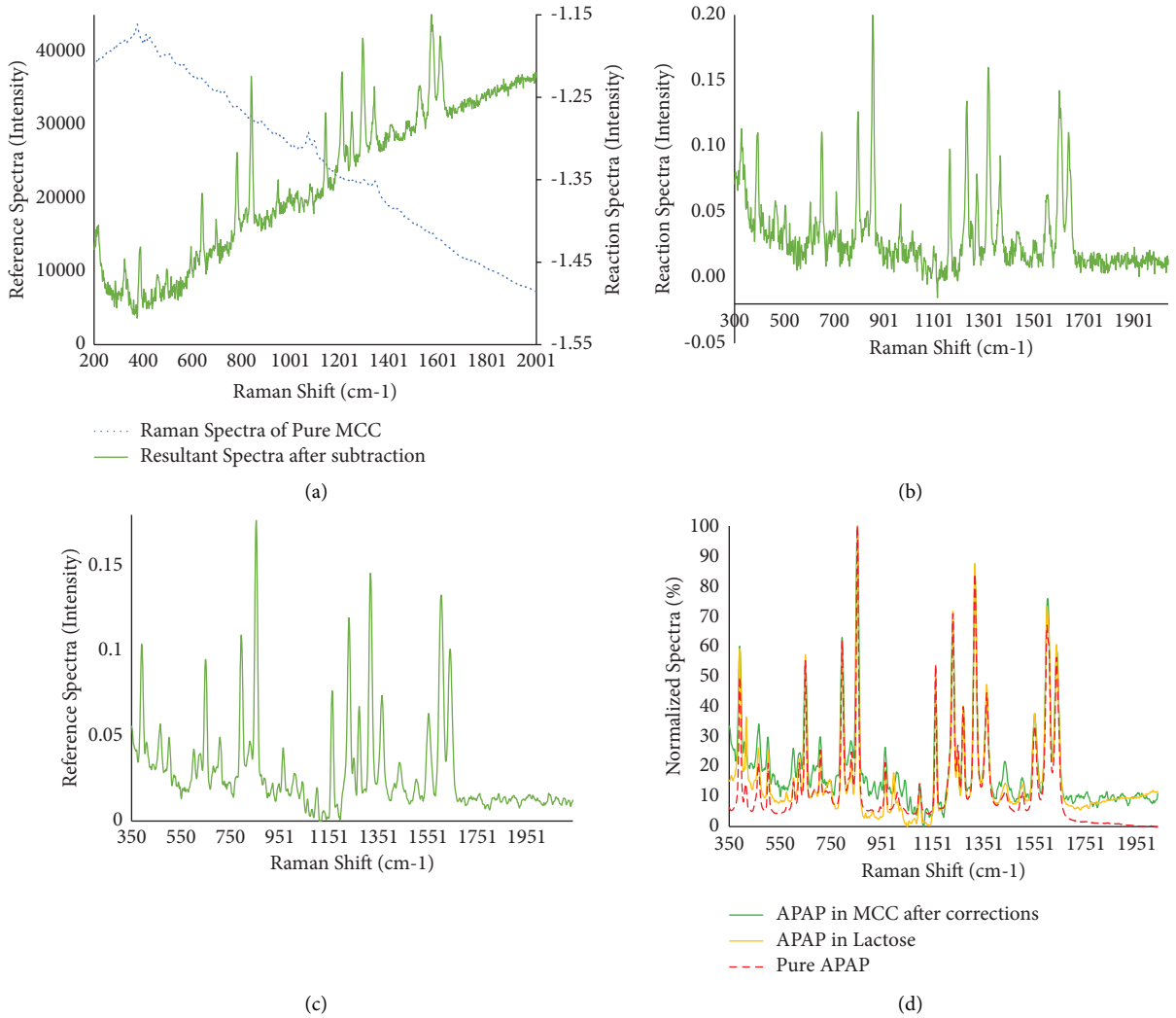

Figure 5: (a) Raman spectra of pure MCC (blue) and resultant spectra after fluorescent material spectra subtraction, (b) Raman spectra after baseline correction, (c) Raman spectra after smoothing, and (d) Raman spectra of 10% APAP in MCC after corrections (green), 10% APAP in lactose (yellow), and pure APAP (red).

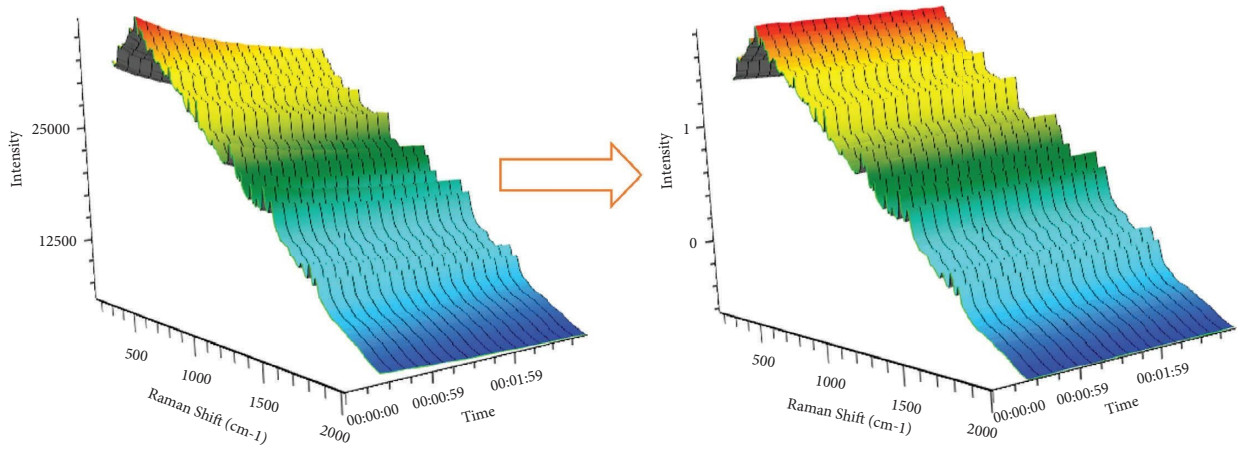

(a)

Figure 6: Continued.

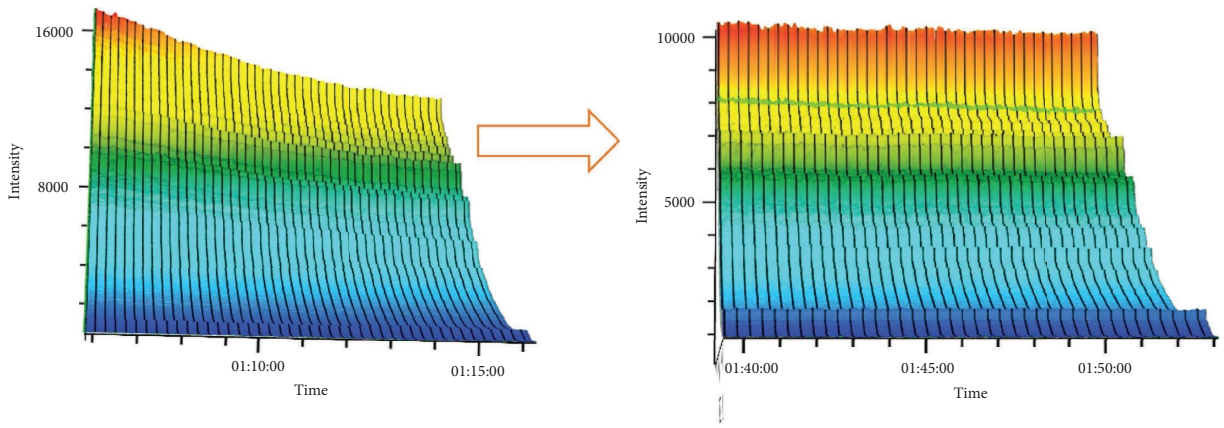

(b)

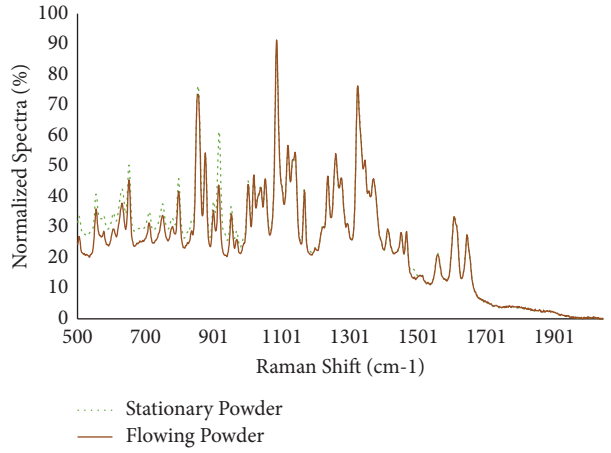

(c)

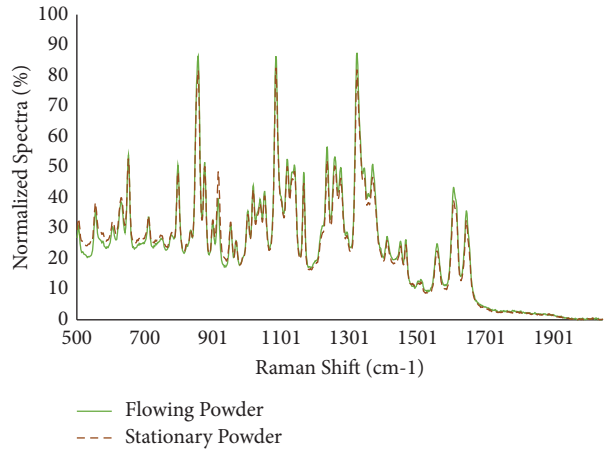

(d)

Figure 6: Continued.

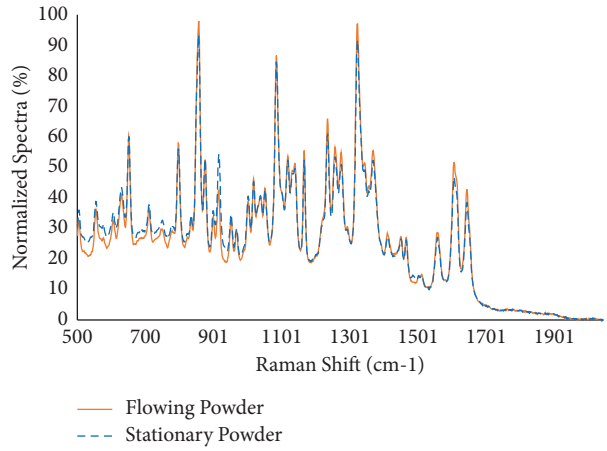

(e)

Figure 6: (a) Surface plot after SNV correction and (b) Raman spectra of stationary powder versus flowing powder at the feed frame; (c–e) Raman spectra of stationary and flowing powder inside the feed frame of tablet press with (c) 8% APAP in lactose, (d) 10% APAP in lactose, and (e) 12% APAP in lactose. Solid lines are Raman spectra of flowing powder and dotted lines are Raman spectra of stationary powder inside the feed frame.

9%, 10%, 11%, 12%, 13%, 14%, and 15%—for model calibration and validation. Material is charged to the hopper of the tablet press and the measurements of the flowing powder are taken at the feed frame by rotating the feed frame at 40 RPM. The raw spectra of all 8 blends and the reference spectra of the main ingredients, APAP and lactose, are shown in Figure 7(a).

Careful examination of these spectra shows that the APAP peaks of the blends are properly coinciding with the APAP peaks in the reference spectra, and that the peak height is varying in accordance with the percentage of APAP charged. These spectral data are then taken to the PLS quantitative toolbox to conduct the multivariate analysis. Multiple models are prepared by adjusting the wavelength ranges and preprocessing steps and the model R-sq values and RMSECV and RMSECP values are compared to find the best model. The wavelength range for the final model is 500 cm^{-1} to 1700 cm^{-1}. The preprocessing techniques applied are spectra averaging, SNV, 2^{nd} derivative, and 11 points smoothing to minimize the RMSECV and RMSEP. Details of the model are given in Figures 7(b)–7(d). The PLS scores indicate that the 8 different blends are clustered away from one another. Only 2 factors are used for this model as they explain more than 98 percent of the variability in data. RMSECV and RMSEP values at 0.351 and 0.286% w/w, respectively, are very good.

The model is then tested by charging a blend with known 10% w/w APAP composition into the feed frame of the tablet press. The predictions of the model in real-time are quite good and are close to the known blend composition of 10% w/w, varying from 9.8% w/w to 10.2% w/w (Figure 8(a)).

3.5.2. PLS Model for acetaminophen in Lactose Using Stationary Powder. In the second set of experiments, the APAP concentration is varied with the main excipient being Lactose. The following APAP concentration blends are used in lactose: 8%, 9%, 10%, 11%, 12%, and 13% APAP (w/w%). The blends are charged to the hopper of the tablet press and the measurements of stationary powder are taken at the feed frame. The details of the model prepared using the measurements on static material are shown in Figures 8(b) and 8(c). R^2 training and R^2 cross-validation values are 0.99 and 0.98, respectively. The number of factors considered are 4, and the RMSECV and RMSEP values are 0.448 and 0.39% w/w, respectively.

Prediction of known APAP concentration (10% w/w) in real-time from the models using flowing powder and stationary powders in the calibration is shown below. Both models performed very well, with the predictions quite close to 10% w/w (Figure 9).

3.5.3. PLS Model for acetaminophen in MCC (Fluorescent Material). As shown above, the model performance using stationary powders is quite good. For this study, the APAP concentration is varied with the fluorescent MCC and the measurement are taken at the stationary powder only. All the blends have the fluorescent background as reported in earlier sections as well. As the excipient imparts fluorescence, preprocessing steps are carried out as explained in Section 3.2 to reduce the impact of fluorescent background. The raw spectra is SNV corrected, Raman spectra of MCC is subtracted, and then baseline correction, smoothing, and normalization are performed. The spectra of different blends and reference material are shown in Figure 10(a). The peak height increases in accordance with the API concentration.

The performance of the resulting PLS model is good and similar to previous cases, as shown in Table 3, even though the raw spectra in all the calibration blends had a significant level of fluorescence interference. The R^2 values of the training and cross validation data set are 0.99 and 0.97, respectively (Figures 10(b) and 10(c)). The RMSECV and RMSEP values at 0.59 and 0.572% w/w, respectively, though slightly higher than the previous two cases, are still good.

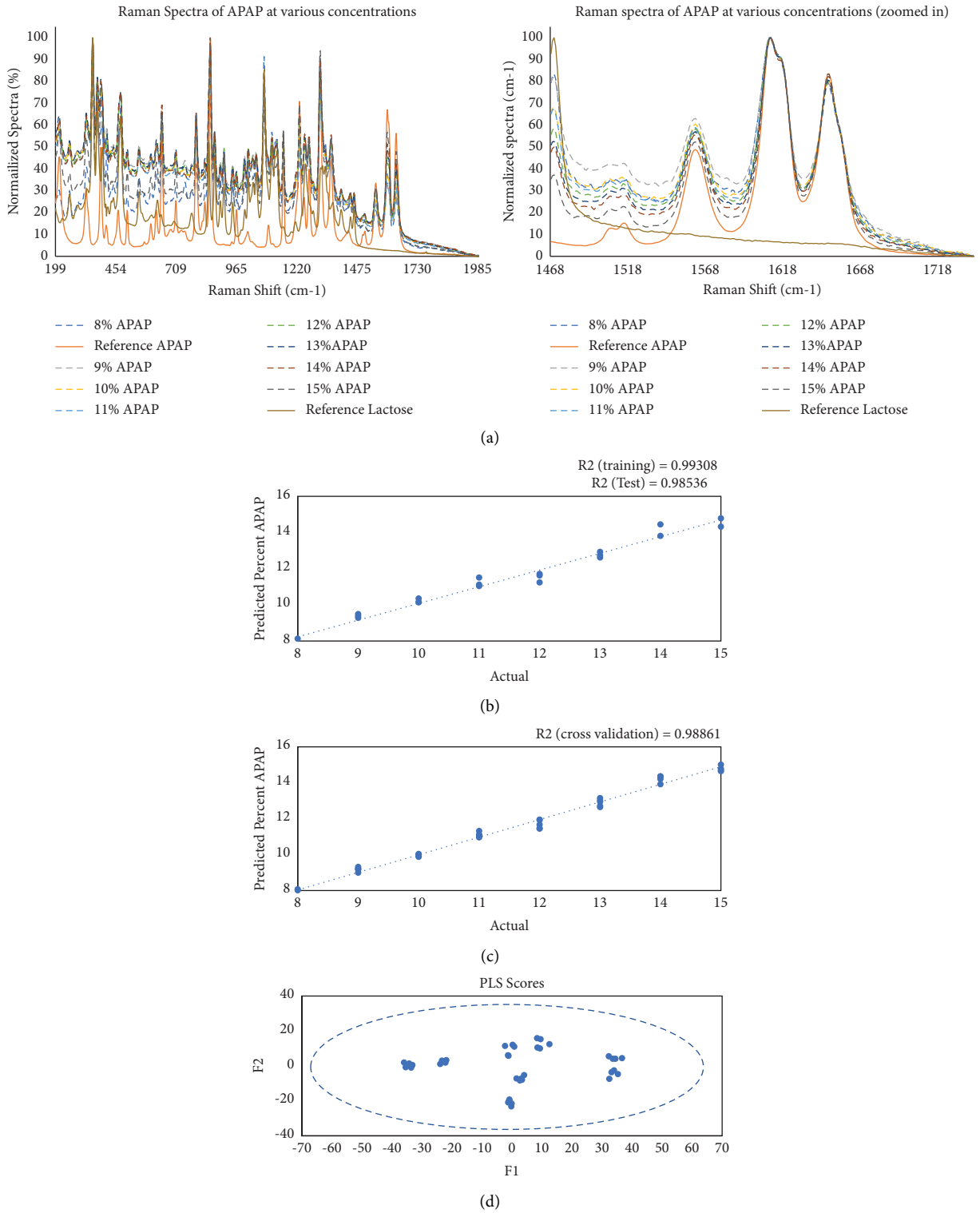

Figure 7: (a) Raman spectra of 8 blends and reference spectra of APAP in lactose, (b) predicted vs. actual training, (c) predicted vs. actual cross -validation, and (d) PLS scores.

3.6. Impact of RPM of Rotating Paddles inside Feed Frame on Model Predictions. To understand the impact of varying RPM of paddles inside feed frame on the predictions of prepared models, powdered blend of 10% w/w APAP and 90% w/w lactose is charged into the feed frame, and the paddle speed is varied from 40 RPM to 20 RPM and then finally to 60 RPM. The predictions are shown in Figure 10(d). The model predictions from both models prepared in Sections 3.5.1 and 3.5.2 show that the predictions are not directly affected by the change in feed frame

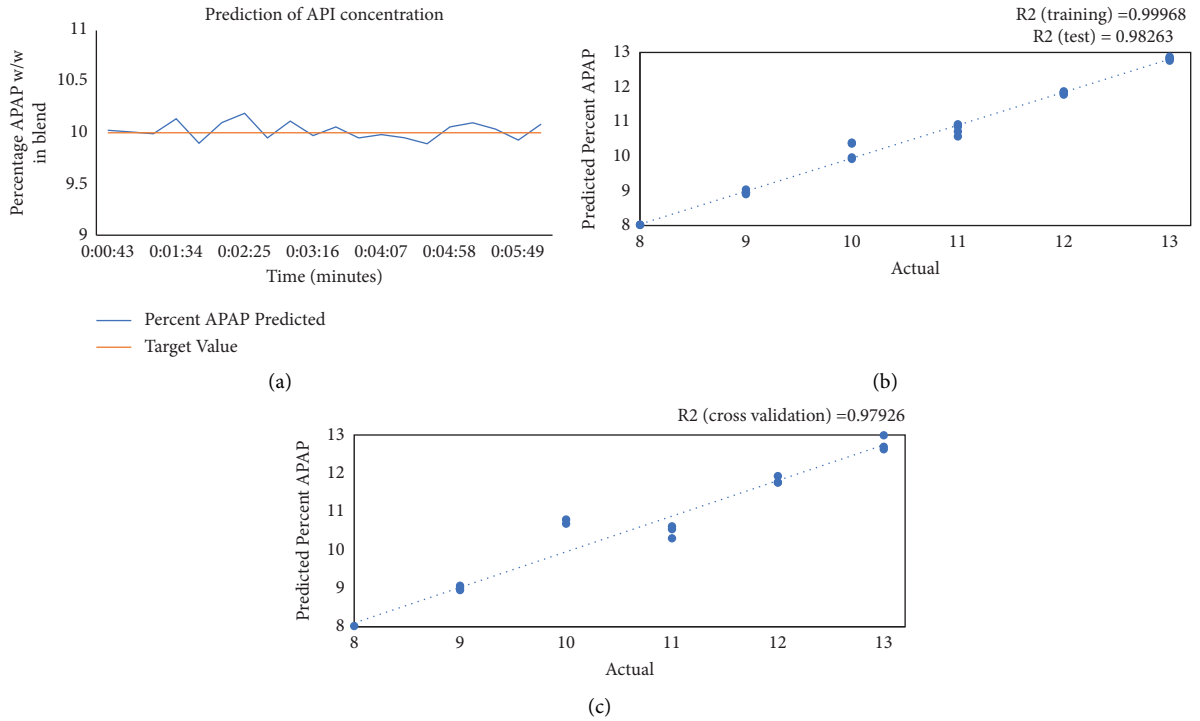

Figure 8: (a) Model predicted vs. Actual APAP concentration at feed frame of tablet press, (b) predicted vs. actual training for APAP in lactose, and (c) predicted vs. actual cross -validation for APAP in lactose.

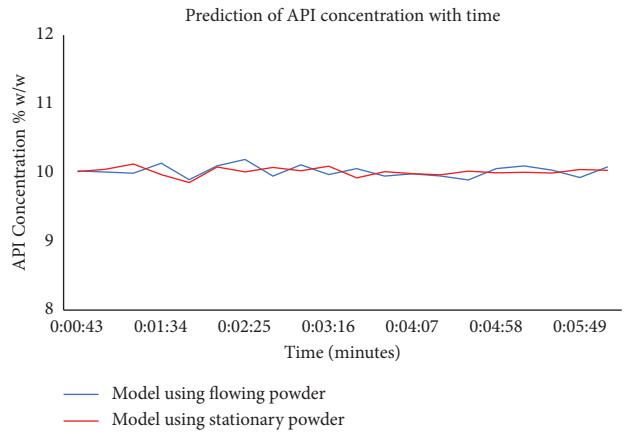

Figure 9: Prediction of API concentration using the model that uses stationary powder data and model that uses flowing powder data against the known concentration of 10% w/w APAP in Lactose.

paddle RPM. This is anticipated as well because in Section 3.4 it was shown that the movement of powders did not affect the Raman spectra much.

4. Discussion

As shown in this work, the presence of one or more fluorescent ingredients in a blend of multiple powder components can obscure the Raman spectra, and depending on the fluorescent background, the important Raman peaks of interest can be masked. Moreover, the fluorescence phenomena are subject to the photobleaching effect as well. However, both the fluorescence and the photobleaching effects can be mitigated through suitable steps as shown by this novelty approach. This has practical implications in that it makes is possible to work with available lasers and not require lasers with different wavelengths to accommodate various excipients and API that may arise in practice.

The comparison of Raman spectra of stationary and powder flowing at different rpm indicated that flow effects do not compromise the quality of the signal. The Raman spectra of MCC of two different grades at different particle sizes was also the same. While we have not reported spectra with the API at different particle sizes, it can be expected that likewise, API particle size variations will not affect the Raman signal. This observed signal stability in the presence of modest variations in

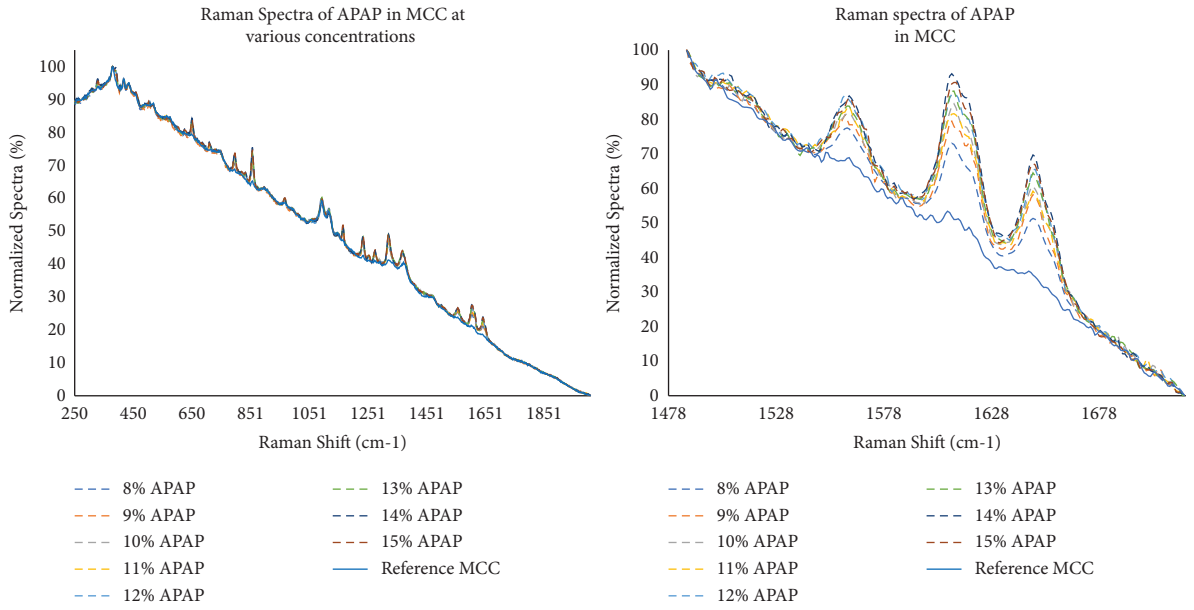

(a)

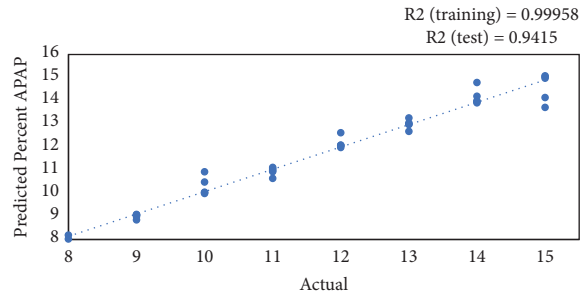

(b)

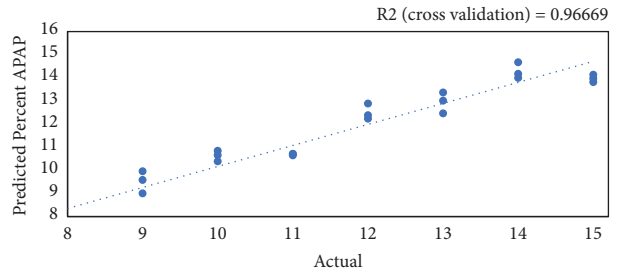

(c)

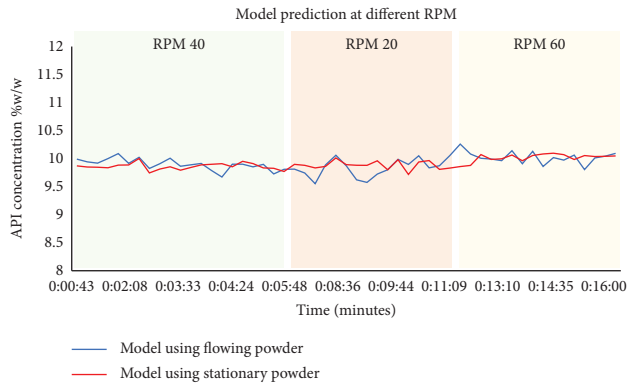

(d)

Figure 10: (a) Raman spectra of blends of API (8%, 9%, 10%, 11%, 12%, 13%, 14%, and 15%) in MCC, (b) predicted vs. actual training for APAP in MCC, (c) predicted vs. actual cross validation for APAP in MCC, and (d) predictions from PLS models at varying feeder RPM of feed frame.

Table 3: Comparison of PLS models.

Model performance parameters	Model comparison		
	APAP in lactose (flowing powder)	APAP in lactose (stationary powder)	APAP in MCC (stationary powder)
R2 training	0.9931	0.9997	0.9996
R2 cross-validation	0.9886	0.9793	0.9667
RMSEC	0.187	0.329	0.0482
RMSECV	0.351	0.448	0.59
RMSEP (%w/w)	0.286	0.39	0.572

the physical state of the material is important as it suggests that such variations will not compromise the key composition CQA.

The favorable comparison of the performance of the PLS models prepared using static and dynamic powder at feed frame has practical implications for situations when not much sample is available. The spectra collection using static samples requires much less material than would be required for flow experiments. The alternative way of taking spectra of flowing powder inside the feed frame and reusing most of the material was also presented and this can be an effective material sparing strategy.

The model using static materials in two scenarios are prepared—APAP in lactose that does not have the fluorescent interference and APAP in MCC where the Raman spectra of the calibration blend suffer from fluorescence. By performing appropriate preprocessing steps, a satisfactory PLS model can be prepared even with the set of blends that has a high level of fluorescence background as shown in Table 3. The performance, although, is better in the APAP in lactose case where the spectra have clearly distinct peaks and have less noise. Changing the RPM of the feed frame did not affect the model predictions when the known quantity of APAP (10% w/w) in lactose is tested at 20, 40, and 60 RPM.

One potential drawback of the Raman instrument used in this work for real-time process monitoring applications is that the sampling time (time for spectra collection plus the time for spectra processing) is more than 7 seconds. Depending on the process dynamics, this might be too long of a period between recorded CQA values for some advanced process control applications and material tracking methods where the time between CQA values of less than a couple of seconds may be desirable. However, this can be mitigated through the use of predictive models to span the period between the recording of CQA values.

5. Conclusion

In this study, the use of Raman spectra at the feed frame of the tablet press was demonstrated. Raman spectroscopy has its own salient features as it provides a unique molecular fingerprint and offers better chemical specificity and hence its implementation is gaining increased acceptance. However, the raw spectra are often affected by fluorescence interference. In the current study, microcrystalline cellulose was observed to be fluorescent in nature for the 785 nm wavelength laser used and the fluorescent interference was present in the blends as well when the MCC concentration was varied from 40% w/w to 90% w/w. However, the raw spectra can still be used to derive the characteristic peaks of material of interest and can be used for building statistical prediction models by following appropriate preprocessing steps. Preprocessing steps should be carefully executed to make sure that the peaks of interest, such as API peaks, in this case, are not eliminated during the process. Other techniques to get rid of fluorescence background were not explored in this study. One unique way of collecting Raman spectra of flowing powder at the feed frame of tablet press is to run the feed frame at the required paddle speed without running the turret. This helps in collecting as many Raman spectra as required with limited materials. Also, as the Raman spectra of stationary and flowing powder are similar and predictions from both cases were comparable, static samples can also be considered for calibration and validation of PLS models to get started until enough material is available to perform the calibration and validation on running the tablet press. However, the model performance should be verified before implementing on the dynamic scenario as other factors such as intense mixing and segregation can affect the model performance.

Data Availability

The data used to support the findings of this study are included in the article, and any additional data are available from the corresponding author upon request.

Conflicts of Interest

The authors declare that they have no conflicts of interest.

Acknowledgments

The authors thank Dr Reddy's Laboratories Ltd, India, for supporting this research project. The authors would also like to thank Yan-Shu for his support in experiments, Purdue University for providing all the resources needed, and Professor Gintaras Reklaitis, Professor Zoltan Nagy, and Professor Marcial Gonzalez for their guidance. This research was supported by the United States Food and Drug Administration through grant number [1U01FD006487-01].

References

[1] S. L. Lee, T. F. O'Connor, X. Yang et al., "Modernizing pharmaceutical manufacturing: from batch to continuous

production," *Journal of Pharmaceutical Innovation*, vol. 10, no. 3, pp. 191–199, 2015.

[2] Y. S. Huang, S. Medina-González, B. Straiton et al., "Real-time monitoring of powder mass flowrates for plant-wide control of a continuous direct compaction tablet manufacturing process," *Journal of Pharmaceutical Sciences*, vol. 111, no. 1, pp. 69–81, 2022.

[3] M. Ierapetritou and G. R. Fernando Muzzio, "Perspective on the continuous manufacturing of powder-based pharmaceutical processes," *AIChE Journal*, vol. 00, p. 17, 2016.

[4] M. Moreno, J. Liu, Q. Su et al., "Steady-state data reconciliation framework for a direct continuous tableting line," *Journal of Pharmaceutical Innovation*, vol. 14, no. 3, pp. 221–238, 2018.

[5] D. C. Hinz, "Process analytical technologies in the pharmaceutical industry: the FDA's PAT initiative," *Analytical and Bioanalytical Chemistry*, vol. 384, no. 5, pp. 1036–1042, 2006.

[6] Center for Drug Evaluation and Research, *Guidance for industry: PAT, a Framework for innovative pharmaceutical development, manufacturing, and quality assurance*, Food and Drug Administration, Rockville, MD, USA, 2004.

[7] L. Makraduli, P. Makreski, K. Goracinova, S. Stefov, M. Anevska, and N. Geskovski, "A comparative approach to screen the capability of Raman and infrared (mid- and near-) spectroscopy for quantification of low-active pharmaceutical ingredient content solid dosage forms: the case of alprazolam," *Applied Spectroscopy*, vol. 74, no. 6, pp. 661–673, 2020.

[8] S. Sasic and S. Ekins, *Pharmaceutical Applications of Raman Spectroscopy*, Wiley, Hoboken, NJ, USA, 1st edition, 2008.

[9] K. A. Bakeev, Edited by K. A. Bakeev, Ed., Wiley, Hoboken, NJ, USA, 2nd edition, 2010.

[10] K. A. Esmonde-White, M. Cuellar, C. Uerpmann, B. Lenain, and I. R. Lewis, "Raman spectroscopy as a process analytical technology for pharmaceutical manufacturing and bioprocessing," *Analytical and Bioanalytical Chemistry*, vol. 409, no. 3, pp. 637–649, 2016.

[11] N. Jung and M. Windbergs, "Raman spectroscopy in pharmaceutical research and industry," *Physical sciences reviews*, vol. 3, no. 8, 2018.

[12] D. Riolo, A. Piazza, C. Cottini et al., "Raman spectroscopy as a PAT for pharmaceutical blending: advantages and disadvantages," *Journal of Pharmaceutical and Biomedical Analysis*, vol. 149, pp. 329–334, 2018.

[13] S. Romero-Torres, J. Huang, and P. E. Hernandez-Abad, "Practical considerations on PAT analyzer selection - Raman vs. NIR spectroscopy," *American Pharmaceutical Review*, vol. 12, no. 7, pp. 12–19, 2009.

[14] Y. Li, C. A. Anderson, J. K. Drennen, C. Airiau, and B. Igne, "Method development and validation of an inline process analytical technology method for blend monitoring in the tablet feed frame using Raman spectroscopy," *Analytical Chemistry*, vol. 90, no. 14, pp. 8436–8444, 2018.

[15] R. S. Das and Y. K. Agrawal, "Raman spectroscopy: recent advancements, techniques and applications," *Vibrational Spectroscopy*, vol. 57, no. 2, pp. 163–176, 2011.

[16] B. Li, A. Calvet, Y. Casamayou-Boucau, C. Morris, and A. G. Ryder, "Low-content quantification in powders using Raman spectroscopy: a facile chemometric approach to sub 0.1% limits of detection," *Analytical Chemistry*, vol. 87, no. 6, pp. 3419–3428, 2015.

[17] P. Allan, L. J. Bellamy, A. Nordon, D. Littlejohn, J. Andrews, and P. Dallin, "In situ monitoring of powder blending by non-invasive Raman spectrometry with wide area illumination," *Journal of Pharmaceutical and Biomedical Analysis*, vol. 76, pp. 28–35, 2013.

[18] D. S. Hausman, R. T. Cambron, and A. Sakr, "Application of Raman spectroscopy for on-line monitoring of low dose blend uniformity," *International Journal of Pharmaceutics*, vol. 298, no. 1, pp. 80–90, 2005.

[19] Y. Kang, Y. Zhou, Q. Wu, N. Wang, and J. Zhou, "Low-content quantitation in entecavir tablets using 1064 nm Raman spectroscopy," *Journal of Spectroscopy*, vol. 2020, Article ID 1308385, 11 pages, 2020.

[20] Z. Y. Zhang, "Rapid discrimination of cheese products based on probabilistic neural network and Raman spectroscopy," *Journal of Spectroscopy*, vol. 2020, Article ID 8896535, 7 pages, 2020.

[21] C. Ortega-Zúñiga, C. P. la Rosa, A. D. Román-Ospino, A. Serrano-Vargas, R. J. Romañach, and R. Méndez, "Development of near infrared spectroscopic calibration models for in-line determination of low drug concentration, bulk density and relative specific void volume within a feed frame," *Journal of Pharmaceutical and Biomedical Analysis*, vol. 164, pp. 211–222, 2019.

[22] Z. D. Harms, Z. Shi, R. A. Kulkarni, and D. P. Myers, "Characterization of near-infrared and Raman spectroscopy for in-line monitoring of a low-drug load formulation in a continuous manufacturing process," *Analytical Chemistry*, vol. 91, no. 13, pp. 8045–8053, 2019.

[23] T. Vankeirsbilck, A. Vercauteren, W. Baeyens et al., "Applications of Raman spectroscopy in pharmaceutical analysis," *TrAC, Trends in Analytical Chemistry*, vol. 21, no. 12, pp. 869–877, 2002.

[24] B. Nagy, A. Farkas, E. Borbás, P. Vass, Z. K. Nagy, and G. Marosi, "Raman spectroscopy for process analytical technologies of pharmaceutical secondary manufacturing," *AAPS PharmSciTech*, vol. 20, no. 1, 2019.

[25] T. de Beer, A. Burggraeve, M. Fonteyne, L. Saerens, J. P. Remon, and C. Vervaet, "Near infrared and Raman spectroscopy for the in-process monitoring of pharmaceutical production processes," *International Journal of Pharmaceutics*, vol. 417, no. 1-2, pp. 32–47, 2011.

[26] J. M. Moran-Mirabal, "The study of cell wall structure and cellulose-cellulase interactions through fluorescence microscopy," *Cellulose*, vol. 20, no. 5, pp. 2291–2309, 2013.

[27] F. C. Thorley, K. J. Baldwin, D. C. Lee, and D. N. Batchelder, "Dependence of the Raman spectra of drug substances upon laser excitation wavelength," *Journal of Raman Spectroscopy*, vol. 37, no. 1-3, pp. 335–341, 2006.

[28] P. George, *Rayleigh and Raman Scattering*, Lawrence Radiation Laboratory, Berkeley, CA, USA, 1962.

[29] M. T. Gebrekidan, C. Knipfer, F. Stelzle, J. Popp, S. Will, and A. Braeuer, "A shifted-excitation Raman difference spectroscopy (SERDS) evaluation strategy for the efficient isolation of Raman spectra from extreme fluorescence interference," *Journal of Raman Spectroscopy*, vol. 47, no. 2, pp. 198–209, 2016.

[30] S. Challa and R. Potumarthi, "Chemometrics-based process analytical technology (PAT) tools: applications and adaptation in pharmaceutical and biopharmaceutical industries," *Applied Biochemistry and Biotechnology*, vol. 169, no. 1, pp. 66–76, 2012.